HALL EFFECT ON MHD MIXED CONVECTION FLOW OF A VISCOELASTIC FLUID PAST AN INFINITE VERTICAL POROUS PLATE WITH MASS TRANSFER AND RADIATION

R.C. CHAUDHARY, P. JAIN

Department of Mathematics, University of Rajasthan
(Jaipur 302004, India; e-mail: jainpreeti28@rediffmail.com)

UDC 532

The unsteady hydromagnetic flow of a viscoelastic fluid from a radiative vertical porous plate has been studied, taking the effect of Hall currents and mass transfer into account. The resulting problem has been solved analytically and the closed form solutions are obtained for velocity, temperature, and concentration distributions, as well as for the shearing stress and rates of heat and mass transfer at the wall. The influence of various parameters like the Hall parameter, magnetic parameter, viscoelastic parameter, frequency parameter, etc. on the flow field is examined.

1. Introduction

Natural convection induced by the simultaneous action of buoyancy forces resulting from thermal and mass diffusion is of considerable interest in many industrial applications such as geophysics, oceanography, drying processes, and solidification of binary alloy. The effect of the magnetic field on free convection flows is important in liquid metals, electrolytes, and ionized gases. The thermal physics of MHD problems with mass transfer is of interest in power engineering and metallurgy. Many cross galvano and thermo-magnetic effects occur in the boundary zone between hydraulics and thermal physics, and they are relevant in the study of semiconductor materials. The mechanism of conduction in ionized gases in the presence of a strong magnetic field is different from that in a metallic substance. The electric current in ionized gases is generally carried by electrons which undergo successive collisions with other charged or neutral particles. In the ionized gases, the current is not proportional to the applied potential except when the electric field is very weak. However, in the presence of strong electric field, the electrical conductivity is affected by the magnetic field. Consequently, the conductivity parallel to the electric field is reduced. Hence, the current is reduced in the direction normal to both electric and magnetic fields. This phenomenon is known as the Hall Effect. The effect of magnetic field (without the Hall effect) on the unsteady free convection flow over an infinite vertical porous plate has been considered in [1, 2]. The effect of a Hall current on the unsteady MHD free convection flow along a vertical porous plate has been studied in [3–7]. The unsteady free convection flow over an infinite vertical porous plate due to the combined effects of thermal and mass diffusion along with Hall currents has been considered in [8–10].

All the above investigations are restricted to MHD flow and heat transfer problems. However, when free convective flows occur at high temperatures, radiation effects on the flow become significant. Many processes in engineering areas occur at high temperatures, and knowledge of radiative heat transfer becomes very important for the design of the pertinent equipment. Nuclear power plants, gas turbines, and the various propulsion devices for aircraft, missiles, and space vehicles are examples of such engineering areas. The inclusion of radiation effects in the energy equation leads to a highly non-linear partial differential equation. The effects of radiation on the free convection flow of a gas past a semiinfinite plate were studied in [11] by using the Cogley–Vincentine–Giles equilibrium model, and those on the MHD free convection flow past a semiinfinite vertical plate were investigated in [12]. The radiation effect on mixed convection along an isothermal vertical plate was studied in [13] with the use of the Rosseland approximation, while this problem was discussed in [14] within the Cogley–Vincentine–Giles equilibrium model. Recently, the heat and mass transfer effects on a moving vertical plate in the presence of thermal radiation were discussed in [15]. In [16], the heat and mass transfer in a heat generating fluid past a vertical porous plate with the Hall current and radiation absorption was analyzed.

All the studies cited above are confined to the flow of Newtonian fluids. However in reality, most of the liquids used in industrial applications, particularly in polymer processing applications, molten plastics, food stuffs or slurries, display the non-Newtonian behaviour.

In [17], the heat transfer in the forced convection flow of a viscoelastic fluid within Walters's model was investigated. The MHD free convection flow of a viscoelastic fluid past a vertical porous plate was studied in [18], and the radiation effect on the free convection heat transfer flow of a non-Newtonian fluid was considered in [19].

In all these studies, the combined effects of mass and radiative heat transfer of a viscoelastic fluid in addition to Hall currents have not been considered simultaneously. We now propose to study the effect of radiation heat absorption and mass transfer on the flow of a viscoelastic fluid past an infinite vertical porous plate taking the Hall effect into account.

2. Mathematical Analysis

We consider the unsteady free convection flow of a viscous, incompressible, electrically conducting fluid on an infinite vertical permeable plate located at the plane $y^* = 0$. The x^*-axis is chosen along the plate in the upward direction, and the y^*-axis is taken perpendicular to the plate. Hall currents give rise to the Lorentz force in the z^*-direction, which induces a cross flow in that direction. Consequently, the flow field becomes three-dimensional. The z^*-axis is assumed to be normal to the $x^* - y^*$ plane. The fluid is assumed to be gray, emitting, and absorbing heat, but not scattering and subjected to a transversely applied uniform magnetic field of strength B_0. Since the plate is infinite in extent, all the physical quantities are functions of y^* and t^* only. At time $t^* > 0$, the plate is kept at the oscillating temperature and concentration. The equations governing the flow of a fluid together with Maxwell's electromagnetic equations are expressed as

Continuity equation

$$\nabla \cdot \vec{V} = 0, \tag{1}$$

Momentum equation

$$\frac{\partial \vec{V}}{\partial t^*} + (\vec{V} \cdot \nabla)\vec{V} = -\frac{1}{\rho}\nabla P + \nu \nabla^2 \vec{V} + \nabla p_{ij} +$$

$$+ g\beta(T - T_\infty) + g\beta_c(C - C_\infty) + \frac{1}{\rho}(\vec{J} \times \vec{B}), \tag{2}$$

Energy equation

$$\frac{\partial T}{\partial t^*} + (\vec{V} \cdot \nabla)T = \frac{K}{\rho c_p}\nabla^2 T - \frac{1}{\rho c_p}\nabla q_r, \tag{3}$$

Species concentration equation

$$\frac{\partial C}{\partial t^*} + (\vec{V} \cdot \nabla)C = D\nabla^2 C, \tag{4}$$

Generalized Ohm's law

$$\vec{J} = \sigma(\vec{E} + \vec{V} \times \vec{B}) - \frac{\sigma}{en_e}(\vec{J} \times \vec{B} - \nabla P_e), \tag{5}$$

Maxwell's equations

$$\nabla \times \vec{H} = \vec{J}, \quad \nabla \times \vec{E} = 0, \quad \nabla \cdot \vec{B} = 0. \tag{6}$$

Here, $\vec{V}\,(u^*, v^*, w^*)$ is the velocity vector, u*, v^*, and w^* are the velocity components along x^*, y^*, and z^* directions, $\vec{B}\,(0, B_0, 0)$ is the magnetic induction, $\vec{E}\,(E_{x*}, E_{y*}, E_{z*})$ is the electric field vector, E_{x*}, E_{y*}, and E_{z*} are the components of the electric field along x^*, y^*, and z^* directions, $\vec{H}$ is the magnetic field strength vector, $\vec{J}\,(J_{x*}, J_{y*}, J_{z*})$ is the current density vector, J_{x*}, J_{y*}, and J_{z*} are the components of the current density along x^*, y^*, and z^* directions, P is the pressure of fluid, P_e is the electron density, p_{ij} is the stress tensor, q_r is the radiative heat flux, e is the electron charge, n_e is the electron number density, T_∞ is the temperature of the fluid far away from the plate, C_∞ is the species concentration far away from the plate, K is thermal conductivity, c_p is specific heat at constant pressure, ρ is the density, σ is the electrical conductivity, β is the volumetric coefficient of thermal expansion, β_c is the volumetric coefficient of expansion with concentration C, g is the gravitational acceleration, D is the chemical molecular diffusivity, and ν is the kinematic viscosity.

In addition, the analysis is based on the following assumptions:

1. The equation of continuity (1) on integration gives

$$v^* = \text{const} = -v_0, \quad v_0 > 0, \tag{7}$$

where v_0 is the constant normal velocity of suction at the plate.

2. The divergence equation of magnetic field $\nabla \vec{B} = 0$ gives

$$B_{y*} = \text{const} = B_0.$$

By assuming a very small magnetic Reynolds number ($\mathrm{Re}_m = \mu_m \sigma \vec{V} L \ll 1$), the induced magnetic field is neglected in comparison to the applied magnetic field so that $B_{y*} = B_{z*} = 0$, hence $\vec{B} = (0, B_0, 0)$. Here, L is the characteristic length and μ_m is the magnetic permeability.

3. Since no polarization voltage is imposed on the flow field, the electric field vector $\vec{E} = 0$. This then corresponds to the case where no energy is added or extracted from the fluid by the electric field.

4. The equation of conservation of charge $\nabla \cdot \vec{J} = 0$ gives, $J_{y*} =$ constant. Since the plate is not conducting, $J_{y*} = 0$ at the plate and, hence, zero everywhere.

5. Considering the magnetic field strength to be very large the generalized Ohm's law including the Hall current and in the absence of the electric field takes the following relation:

$$\vec{J} + \frac{\omega_e \tau_e}{B_0}(\vec{J} \times \vec{B}) = \sigma \left(\vec{V} \times \vec{B} + \frac{\nabla P_e}{en_e}\right), \tag{8}$$

where ω_e is the Larmor frequency and τ_e is the electron collision time. For weakly ionized gases, the thermoelectric pressure and the ion slip are considered negligible. Equation (8) reduces to

$$J_{x*} = \frac{\sigma B_0}{1+m^2}(mu^* - w^*), \tag{9}$$

$$J_{z*} = \frac{\sigma B_0}{1+m^2}(u^* + mw^*), \tag{10}$$

where $m = \omega_e \tau_e$ is the Hall parameter. Thus, the governing equations of the flow in the usual Boussinesq approximation now become:

Momentum equation

$$\frac{\partial u^*}{\partial t^*} - v_0 \frac{\partial u^*}{\partial y^*} = \nu \frac{\partial^2 u^*}{\partial y^{*2}} -$$

$$-k_0^* \frac{\partial^3 u^*}{\partial y^{*2}\,\partial t^*} - \frac{\sigma B_0^2 (u^* + mw^*)}{\rho(1+m^2)} +$$

$$+g\beta(T - T_\infty) + g\beta_c (C - C_\infty), \tag{11}$$

$$\frac{\partial w^*}{\partial t^*} - v_0 \frac{\partial w^*}{\partial y^*} = \nu \frac{\partial^2 w^*}{\partial y^{*2}} -$$

$$-k_0^* \frac{\partial^3 w^*}{\partial y^{*2}\,\partial t^*} + \frac{\sigma B_0^2 (mu^* - w^*)}{\rho(1+m^2)}, \tag{12}$$

Energy equation

$$\frac{\partial T}{\partial t^*} - v_0 \frac{\partial T}{\partial y^*} = \frac{K}{\rho c_p} \frac{\partial^2 T}{\partial y^{*2}} - \frac{1}{\rho c_p} \frac{\partial q_r}{\partial y^*}, \tag{13}$$

Species concentration equation

$$\frac{\partial C}{\partial t^*} - v_0 \frac{\partial C}{\partial y^*} = D \frac{\partial^2 C}{\partial y^{*2}}. \tag{14}$$

By using [15,21], the local radiant for the case of an optically thin gray gas is expressed as

$$\frac{\partial q_r}{\partial y^*} = -4a_R \sigma^* (T_\infty^4 - T^4). \tag{15}$$

It is assumed that the temperature differences within the flow are significantly small such that T^4 may be expressed as a linear function of the temperature. This is accomplished by expanding T^4 in a Taylor series about T_∞ and neglecting higher order terms. Thus, we have

$$T^4 \approx 4T_\infty^3 T - 3T_\infty^4. \tag{16}$$

By using (15) and (16), the energy equation (13) reduces to

$$\frac{\partial T}{\partial t^*} - v_0 \frac{\partial T}{\partial y^*} = \frac{k}{\rho c_p} \frac{\partial^2 T}{\partial y^{*2}} +$$

$$+\frac{16 a_R \sigma^* T_\infty^3 (T_\infty - T)}{\rho c_p}. \tag{17}$$

Here, a_R is radiation absorption coefficient and σ^* is the Stefan–Boltzmann constant.

In Eq. (13), viscous dissipation and Ohmic dissipation are neglected, and, in Eq. (14), the term due to a chemical reaction is assumed to be absent. The initial and boundary conditions read

$$\left.\begin{array}{l} t^* \le 0 : u^*(y^*, t^*) = w^*(y^*, t^*) = 0 \\ T(y^*, t^*) = 0, \quad C(y^*, t^*) = 0 \end{array}\right\} \text{for all } y^*,$$

$$t^* > 0 : u^* = 0, \quad w^* = 0, \quad T = T_\infty + (T_w - T_\infty) e^{i\omega^* t^*},$$
$$C = C_\infty + (C_w - C_\infty) e^{i\omega^* t^*}$$
$$: u^*(\infty, t^*) = w^*(\infty, t^*) = T(\infty, t^*) = C(\infty, t^*) = 0, \tag{18}$$

where ω^* is the frequency of oscillations, subscripts w and ∞ denote the physical quantities at the plate and in the free stream, respectively. We use the dimensionless parameters

$$\eta = \frac{v_0 y^*}{\nu}, \quad t = \frac{v_0^2 t^*}{4\nu}, \quad \Omega = \frac{4\nu\omega^*}{v_0^2},$$

$$u = \frac{u^*}{v_0}, \quad w = \frac{w^*}{v_0}, \quad \theta = \frac{T - T_\infty}{T_w - T_\infty}, \quad C = \frac{C - C_\infty}{C_w - C_\infty},$$

$$\mathrm{Gr} = \frac{4g\beta\nu(T_w - T_\infty)}{v_0^3}, \quad \mathrm{Gc} = \frac{4g\beta_c\nu(C_w - C_\infty)}{v_0^3},$$

$$M = \frac{4\sigma B_0^2\nu}{\rho v_0^2}, \quad \mathrm{Pr} = \frac{\mu c_p}{k},$$

$$\mathrm{Sc} = \frac{\nu}{D}\ ,\ R = \frac{64\, a_R \sigma^{\,*} \nu^2 T_\infty^3}{k v_0^2}\ ,\ k = \frac{k_0^*\, v_0^2}{\nu^2}. \tag{19}$$

Here, Gr is the Grashof number; Gc is the mass Grashof number; M is the magnetic parameter; Pr is the Prandtl number; Sc is the Schmidt number; R is the radiation parameter; and k is the viscoelastic parameter. Equations (11)–(14) are now transformed to their corresponding dimensionless form as

$$\frac{\partial u}{\partial t} - 4\,\frac{\partial u}{\partial \eta} = 4\frac{\partial^2 u}{\partial \eta^2} - k\frac{\partial^3 u}{\partial \eta^2\,\partial t} - \frac{M}{1+m^2}\,(mw+u) + \mathrm{Gr}\theta + \mathrm{Gc}C, \tag{20}$$

$$\frac{\partial w}{\partial t} - 4\,\frac{\partial w}{\partial \eta} = 4\,\frac{\partial^2 w}{\partial \eta^2} - k\frac{\partial^3 w}{\partial \eta^2 \partial t} + \frac{M}{1+m^2}\,(mu - w), \tag{21}$$

$$\frac{\partial \theta}{\partial t} - 4\,\frac{\partial \theta}{\partial \eta} = \frac{4}{\mathrm{Pr}}\,\frac{\partial^2 \theta}{\partial \eta^2} - \frac{R}{\mathrm{Pr}}\theta, \tag{22}$$

$$\frac{\partial C}{\partial t} - 4\,\frac{\partial C}{\partial \eta} = \frac{4}{\mathrm{Sc}}\,\frac{\partial^2 C}{\partial \eta^2}. \tag{23}$$

The modified boundary conditions become

$$\begin{cases} t \le 0 : u(\eta,t) = w(\eta,t) = \theta\,(\eta,t) = C(\eta,t) = 0, \quad \text{for all } \eta, \\ t > 0 : u(0,t) = w(0,t) = 0, \quad \theta(0,t) = e^{i\Omega t}, \quad C(0,t) = e^{i\Omega t}, \\ u(\infty,t) = w(\infty,t) = \theta\,(\infty,t) = C(\infty,t) \to 0. \end{cases} \tag{24}$$

Equations (20) and (21) can be combined into a single equation by introducing the complex velocity

$$\psi = u + iw, \quad \text{where } i = \sqrt{-1}. \tag{25}$$

We get

$$\frac{\partial^2 \psi}{\partial \eta^2} - \frac{k}{4}\frac{\partial^3 \psi}{\partial \eta^2\,\partial t} - \frac{1}{4}\,\frac{\partial \psi}{\partial t} + \frac{\partial \psi}{\partial \eta} - \frac{M(1-im)\psi}{4(1+m^2)} = -\frac{\mathrm{Gr}\theta}{4} - \frac{\mathrm{Gc}C}{4}. \tag{26}$$

Again, by using Eq. (25), the boundary conditions in Eq. (24) are transformed to

$$\begin{cases} t \le 0 : \psi(\eta,t) = \theta\,(\eta,t) = C(\eta,t) = 0, \quad \text{for all } \eta, \\ t > 0 : \psi(0,t) = 0, \quad \theta(0,t) = C(0,t) = e^{i\Omega t}, \\ \psi(\infty,t) = \theta\,(\infty,t) = C(\infty,t) \to 0. \end{cases} \tag{27}$$

Substituting $\theta\,(\eta,t) = e^{i\Omega t}\, f(\eta)$ in Eq. (22), we get

$$f^{''}(\eta) + \mathrm{Pr} f^{'}(\eta) - \frac{1}{4}(R + i\Omega\mathrm{Pr}) f(\eta) = 0 \tag{28}$$

which has to be solved under the boundary conditions

$$f(0) = 1, \ \ f(\infty) = 0. \tag{29}$$

Hence,

$$f(\eta) = e^{-\frac{\eta}{2}\left[\mathrm{Pr} + \sqrt{\mathrm{Pr}^2 + R + i\Omega\mathrm{Pr}}\right]} \Rightarrow$$

$$\Rightarrow \theta(\eta,t) = e^{i\Omega t - \frac{\eta}{2}\left[\mathrm{Pr} + \sqrt{\mathrm{Pr}^2 + R + i\Omega\mathrm{Pr}}\right]}.$$

Separating the real and imaginary parts, the real part is given by

$$\theta_r(\eta,t) = \left\{\cos\left(\Omega t - \frac{\eta}{2}\, D_1 \sin\frac{\alpha}{2}\right)\right\} e^{-\frac{\eta}{2}\left[\mathrm{Pr} + D_1 \cos\frac{\alpha}{2}\right]}, \tag{30}$$

where

$$D_1 = [(\mathrm{Pr}^2 + R)^2 + \Omega^2 \mathrm{Pr}^2]^{1/4},$$

$$\alpha = \tan^{-1}\left(\frac{\Omega \mathrm{Pr}}{\mathrm{Pr}^2 + R}\right). \tag{31}$$

Now, putting $C(\eta, t) = e^{i\Omega t} g(\eta)$ in Eq. (23), we get

$$g''(\eta) + \mathrm{Sc}\, g'(\eta) - \frac{i\Omega \mathrm{Sc}}{4} g(\eta) = 0, \tag{32}$$

which has to be solved under the boundary condition

$$g(0) = 1, \;\; g(\infty) = 0. \tag{33}$$

Hence,

$$g(\eta) = e^{-\frac{\eta}{2}\left[\mathrm{Sc}^2 + \sqrt{\mathrm{Sc}^2 + i\Omega \mathrm{Sc}}\right]} \Rightarrow$$

$$\Rightarrow C(\eta, t) = e^{i\Omega t - \frac{\eta}{2}\left[\mathrm{Sc}^2 + \sqrt{\mathrm{Sc}^2 + i\Omega \mathrm{Sc}}\right]}.$$

Separating the real and imaginary parts, the real part is given by

$$C_r(\eta, t) = \left\{\cos\left(\Omega t - \frac{\eta}{2} D_2 \sin\frac{\beta}{2}\right)\right\} e^{-\frac{\eta}{2}\left[\mathrm{Sc} + D_2 \cos\frac{\beta}{2}\right]}, \tag{34}$$

where

$$D_2 = [\mathrm{Sc}^2 + \Omega^2]^{1/4} \mathrm{Sc}^{1/2}, \quad \beta = \tan^{-1}\left(\frac{\Omega}{\mathrm{Sc}}\right). \tag{35}$$

In order to solve Eq. (26), we substitute $\psi = e^{i\Omega t} F(\eta)$, and the corresponding boundary conditions now become

$$F(0) = 0, \quad F(\infty) = 0. \tag{36}$$

Separating the real and imaginary parts, we get

$$u = [B_{15} \cos(\Omega t - B_6 \eta) - B_{16} \sin(\Omega t - B_6 \eta)] e^{-B_5 \eta} -$$

$$-[\mathrm{Gr} B_{11} \cos(\Omega t - B_2 \eta) - \mathrm{Gr} B_{12} \sin(\Omega t - B_2 \eta)] e^{-B_1 \eta} -$$

$$-[\mathrm{Gc} B_{13} \cos(\Omega t - B_4 \eta) - \mathrm{Gc} B_{14} \sin(\Omega t - B_4 \eta)] e^{-B_3 \eta}, \tag{37}$$

$$w = [B_{16} \cos(\Omega t - B_6 \eta) + B_{15} \sin(\Omega t - B_6 \eta)] e^{-B_5 \eta} -$$

$$-[\mathrm{Gr} B_{12} \cos(\Omega t - B_2 \eta) + \mathrm{Gr} B_{11} \sin(\Omega t - B_2 \eta)] e^{-B_1 \eta} -$$

$$-[\mathrm{Gc} B_{14} \cos(\Omega t - B_4 \eta) + \mathrm{Gc} B_{13} \sin(\Omega t - B_4 \eta)] e^{-B_3 \eta}. \tag{38}$$

If τ_1 and τ_2 are the axial and transverse components of the skin friction, respectively, then

$$\tau_1 + i\tau_2 = \mu \left(\frac{\partial \psi}{\partial \eta}\right)_{\eta=0}.$$

In the dimensionless form, τ_1 becomes

$$\tau_1 = \left(\frac{\partial u}{\partial \eta}\right)_{\eta=0} = B_5 B_{16} + B_6 B_{15} -$$

$$-\mathrm{Gr}(B_1 B_{12} + B_2 B_{11}) - \mathrm{Gc}(B_3 B_{14} + B_4 B_{13}). \tag{39}$$

Similarly, the shear stress at the wall along the z-axis is given by

$$\tau_2 = \left(\frac{\partial w}{\partial \eta}\right)_{\eta=0} = -B_5 B_{15} + B_6 B_{16} +$$

$$+\mathrm{Gr}(B_1 B_{11} - B_2 B_{12}) + \mathrm{Gc}(B_3 B_{13} - B_4 B_{14}). \tag{40}$$

For the temperature field, the heat transfer coefficient in terms of the Nusselt number is given by

$$\mathrm{Nu} = -\left.\frac{\partial \theta_r(\eta, t)}{\partial \eta}\right|_{\eta=0} =$$

$$= \frac{1}{2}\left[\mathrm{Pr} \cos \Omega t + D_1 \cos\left(\Omega t + \frac{\alpha}{2}\right)\right]. \tag{41}$$

Further, the coefficient of mass transfer for the concentration field in terms of the Sherwood number is given by

$$\mathrm{Sh} = -\left.\frac{\partial C_r(\eta, t)}{\partial \eta}\right|_{\eta=0} =$$

$$= \frac{1}{2}\left[\mathrm{Sc} \cos \Omega t + D_2 \cos\left(\Omega t + \frac{\beta}{2}\right)\right], \tag{42}$$

where

$$B_1 = \frac{1}{2}\left[\mathrm{Pr} + D_1 \cos\frac{\alpha}{2}\right], \quad B_2 = \frac{D_1}{2} \sin\frac{\alpha}{2},$$

$$B_3 = \frac{1}{2}\left[\mathrm{Sc} + D_2 \cos\frac{\beta}{2}\right],$$

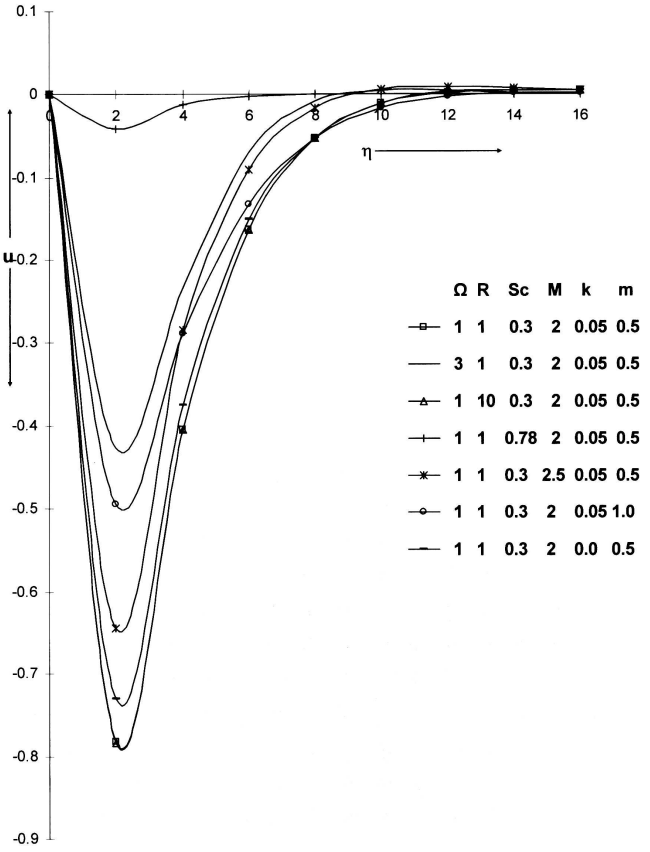

Fig. 1. Variation of velocity component u for Pr = 3.0, Gc = 2.0, Gr = 5.0, $\Omega t = \pi/2$

$$B_4 = \frac{D_2}{2}\sin\frac{\beta}{2}D_3 =$$

$$= \left[\left[1+\frac{M}{1+m^2}-\frac{k\Omega}{4}\left(\frac{Mm}{1+m^2}-\Omega\right)\right]^2 +\right.$$

$$\left.+\left[\Omega-\frac{4Mm+k\Omega M}{4(1+m^2)}\right]^2\right]^{1/4},$$

$$\gamma = \tan^{-1}\left[\frac{\Omega-\left(\frac{4Mm+k\Omega M}{4(1+m^2)}\right)}{1+\frac{M}{1+m^2}-\frac{k\Omega}{4}\left(\frac{Mm}{1+m^2}-\Omega\right)}\right],$$

$$D_4 = k\Omega/4,$$

$$B_5 = \frac{1+D_3\left(\cos\frac{\gamma}{2}-D_4\sin\frac{\gamma}{2}\right)}{2(1+D_4^2)},$$

$$B_6 = \frac{D_4+D_3\left(D_4\cos\frac{\gamma}{2}+\sin\frac{\gamma}{2}\right)}{2(1+D_4^2)},$$

$$B_7 = 4(B_1^2-B_2^2)+2B_1B_2k\Omega+4B_1-\frac{M}{1+m^2},$$

$$B_8 = (B_1^2-B_2^2)k\Omega-8B_1B_2-4B_2+\Omega-\frac{Mm}{1+m^2},$$

$$B_9 = 4(B_3^2-B_4^2)+2k\Omega B_3B_4+4B_3-\frac{M}{1+m^2},$$

$$B_{10} = -8B_3B_4+k\Omega(B_3^2-B_4^2)-4B_4+\Omega-\frac{Mm}{1+m^2},$$

$$B_{11} = \frac{B_7}{B_7^2+B_8^2}, \quad B_{12} = \frac{B_8}{B_7^2+B_8^2},$$

$$B_{13} = \frac{B_9}{B_9^2+B-10^2}, \quad B_{14} = \frac{B_{10}}{B_9^2+B_{10}^2},$$

$$B_{15} = \mathrm{Gr}B_{11}+\mathrm{Gc}B_{13}, \quad B_{16} = \mathrm{Gr}B_{12}+\mathrm{Gc}B_{14}.$$

3. Discussion and Conclusion

In order to illustrate the influence of various parameters on the velocity, temperature, concentration fields, shear stress, and rates of heat and mass transfer, we have carried out the numerical calculations of the solutions obtained in the preceding section. The Prandtl number is taken to be equal to 3, which physically corresponds to Freon. Freon represents several different chlorofluorocarbons or CFCs which are used in commerce and industry.

Figure 1 depicts the primary velocity profiles u against η taking different values of Ω (frequency), R (radiation parameter), Sc (Schmidt number), M (magnetic parameter), k (viscoelastic parameter), and m (Hall parameter). It is seen from Fig. 1 that the effect of increasing the magnetic parameter and frequency is to enhance the primary velocity. Also the magnitude of primary velocity is greater for helium (Sc = 0.30, at 25 °C temperature and a pressure of 1 atm.) than for ammonia (Sc = 0.78, at 25 °C temperature and a pressure of 1 atm. This figure further indicates that the primary velocity increases with the Hall parameter.

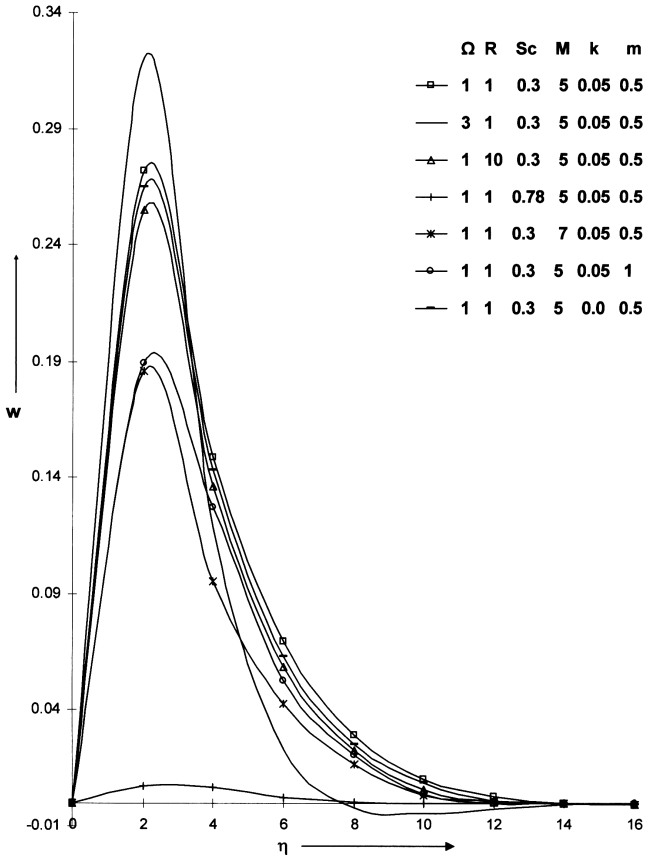

Fig. 2. Variation of velocity component w for Pr = 3.0, Gc = 2.0, Gr = 5.0, $\Omega t = \pi/2$

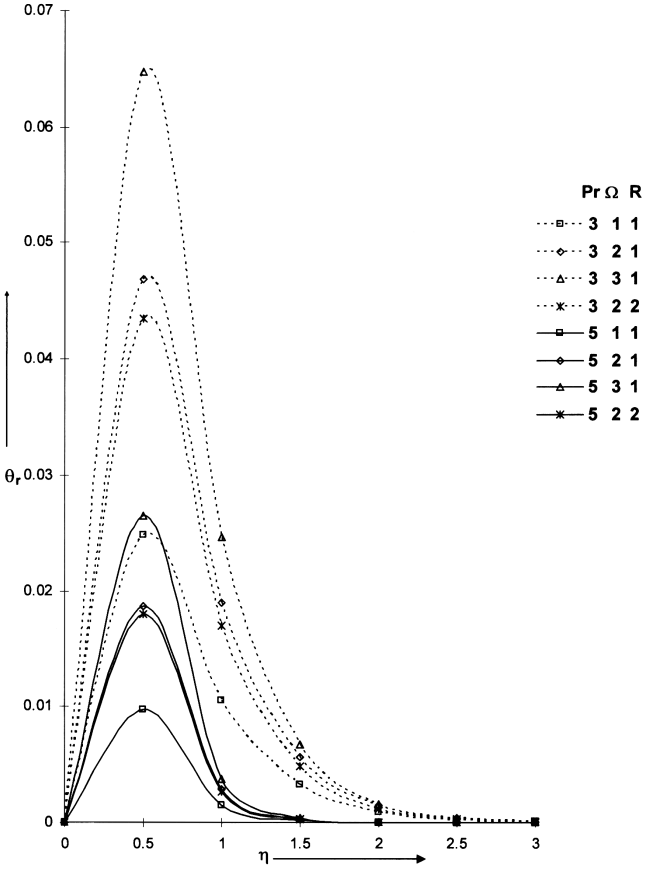

Fig. 3. Variation of temperature θ_r

Moreover, the velocity of a Newtonian fluid ($k = 0$) is more than the velocity of a non-Newtonian fluid ($k \neq 0$). On increasing the radiation parameter (R), the values of u differed only by small amounts, therefore the curves could not be shown distinctly in Fig. 1.

The secondary velocity profiles w for the cooling of the plate are plotted in Fig. 2. The analysis of the graph reveals that, on increasing the values of the frequency (Ω) parameter, a sharp rise in the magnitude of velocity profile is observed near the plate. But, at a certain distance away from the plate, it falls rapidly and finally decays to the free-stream value. A close examination of the data presented in Fig. 2 shows that the radiation parameter tends to reduce the fluid velocity in secondary flows. The retardation in the secondary velocity field due to the increase in the magnetic and Hall parameters is also noticed form this figure. This observation can be explained by the following fact. As M increases, the Lorentz force, which opposes the flow, also increases and leads to the enhanced deceleration of the flow. The velocity of helium is greater than the velocity of ammonia in secondary flows. Further, it is apparent that the w-component of velocity of a Newtonian fluid is lower than that of a viscoelastic fluid. Finally, it turns out that the maximum velocity occurs in the vicinity of the plate, and, as $\eta \to \infty$, the velocity profiles terminate to zero.

Figure 3 represents the temperature profiles θ_r against η for different values of Pr, Ω, and R taking $\Omega t = \pi/2$. In the neighborhood of the surface, the temperature profiles become maximum and then decrease and finally take asymptotic values. The thermal boundary layer thickness is greater for fluids with small Prandtl number. The reason is that smaller values of Pr are equivalent to increasing the thermal conductivity, and therefore heat is able to diffuse away from the heated surface more rapidly than for higher values of Pr. It is observed that the temperature rises with increasing the frequency while the reverse happen for increasing values of the radiation parameter.

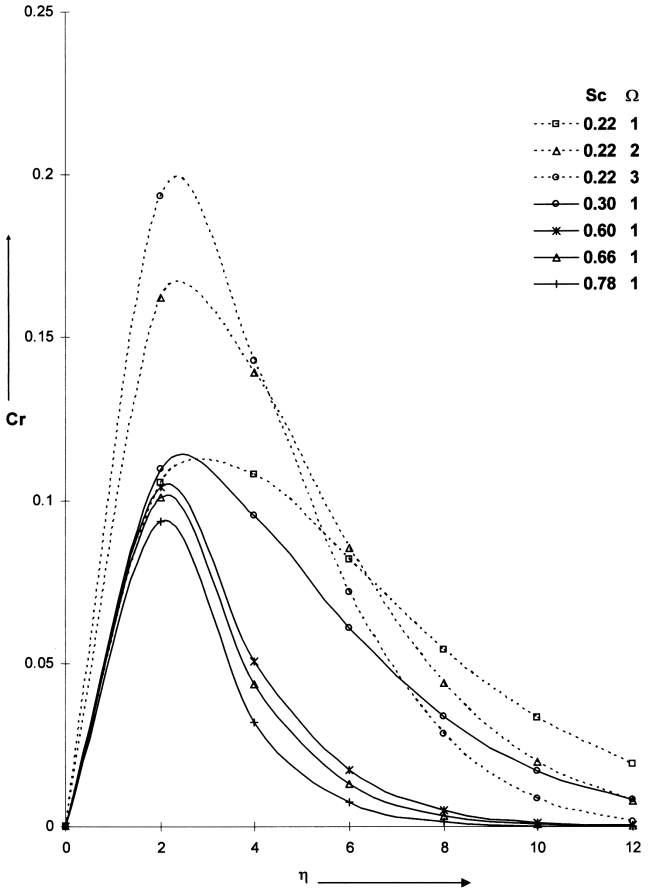

Fig. 4. Variation of concentration Cr

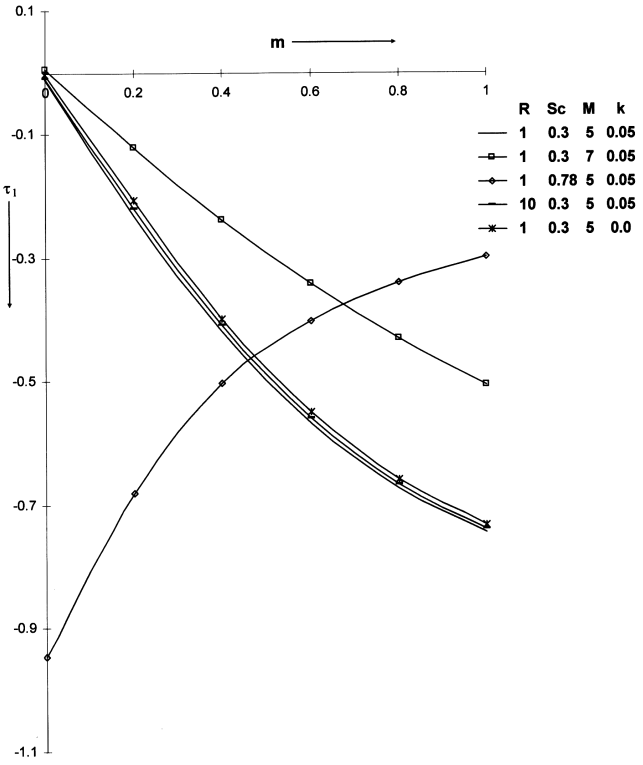

Fig. 5. Variation of shearing stress τ_1 for Pr = 3.0, Gr = 5.0, Gc = 2.0, $\Omega = 1.0$, $\Omega t = \pi/2$

Figure 4 displays the concentration profiles Cr vs η for various gases like hydrogen (Sc = 0.22), helium (Sc = 0.30), water vapor (Sc = 0.60), oxygen (Sc = 0.66), and ammonia (Sc = 0.78) taking $\Omega t = \pi/2$. It is reported that the effect of increasing the Schimdt number (Sc) is to decrease the concentration profiles. This is consistent with the fact that the increase of Sc means a decrease of molecular diffusivity (D), which results in a decrease of the concentration boundary layer. Hence, the concentration of species is higher for smaller value of Sc and lower for larger value of Sc. Furthermore, it is observed that the thickness of the concentration boundary layer increases significantly near the boundary with increase in the frequency, but the opposite trend is noted far away from the plate ($\eta > 4$).

Figure 5 elucidates the effects of R, Sc, M, and k on the shear stress along the x-axis, τ_1, while the shear stress along the z-axis, τ_2, is shown in Fig. 6. The axial and transverse components of the skin friction are plotted against the Hall parameter. It is observed that, for Sc = 0.30, both τ_1 and τ_2 decrease with increase in m. But, for Sc = 0.78, the shear stress along the x- and z-axes increases with increase in m. Further, since the velocity in primary flows increases with increase in M, τ_1 also increases with M, because the friction increases with the fluid velocity. Similarly, the velocity in secondary flows decreases as M increases. Therefore, τ_2 also exhibits a similar behaviour as M increases. Due to the increase in R, the velocity gradient in primary flows increases, but the velocity gradient in secondary flows decreases. Finally, it is seen that the transverse component of skin friction τ_2 is lower for a non-Newtonian fluid as compared to a Newtonian fluid. But the opposite trend is noted for the axial component of skin friction τ_1. Figures 5 and 6 reveal that since the Hall parameter (m) gives rise to the secondary flow field, the transverse component of skin friction is greater than the axial component of skin friction at and near the wall.

The quantity of heat exchanged between the body and the fluid is given by the temperature gradient Nu (Nusselt number) which is given below in Table 1.

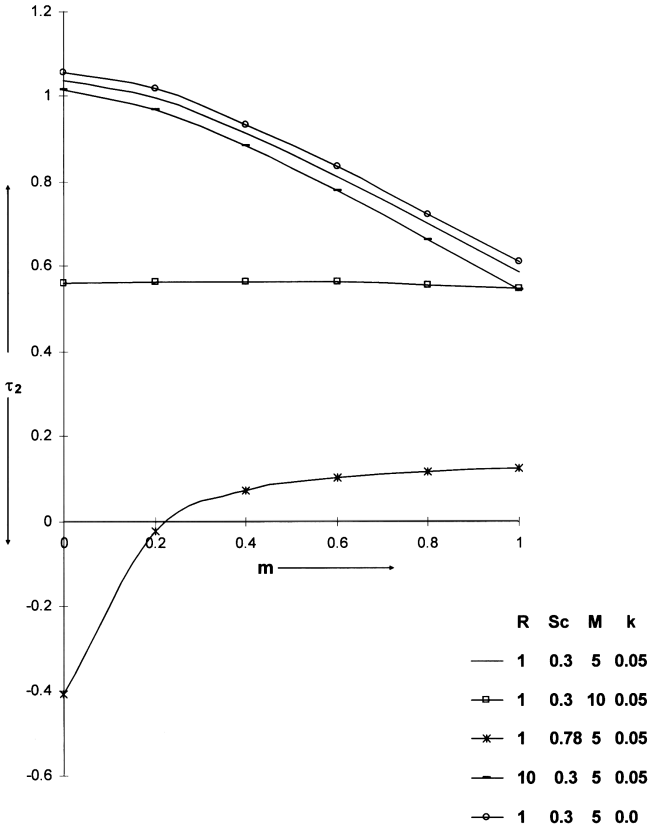

Fig. 6. Variation of shearing stress τ_2 for Pr = 3.0, Gr = 5.0, Gc = 2.0, $\Omega = 1.0$, $\Omega t = \pi/2$

It is inferred that the higher values of frequency and radiation parameter increase the magnitude of temperature gradient. The rate of mass transfer Sh (Sherwood number) for different values of Sc and Ω is shown below in Table 2.

From Table 2, it is revealed that the magnitude of Sh increases with Sc and Ω since an increase in Sc causes a reduction in concentration boundary layers. Therefore, the rate of mass transfer increases with Sc.

T a b l e 1. Rate of heat transfer (Nu)

	Nu	
Ω	R	Pr = 3.0
1.0	1.0	–1.5984
2.0	1.0	–1.6455
3.0	1.0	–1.7122
1.0	2.0	–1.67338

T a b l e 2. Rate of mass transfer (Sh)

	Sh		
Ω	Sc = 0.22	Sc = 0.30	Sc = 0.78
1.0	–0.21449	–0.25104	–0.4292
2.0	–0.2793	–0.3257	–0.5292
3.0	–0.3275	–0.3819	–0.61605
4.0	–0.3682	–0.4295	–0.69189

1. G.A. Georgantopoulos, J. Koullias, C.L. Goudas, and C. Courogenis, Astrophys. Space Sci. **74**, 357 (1981).
2. K.A. Helmy, ZAMM **78**, 225 (1999).
3. M. Katagiri, J. Phys. Soc. Jpn. **27**, 1051 (1969).
4. M.A. Hossain, J. Phys. Soc. Jpn. **55**, 2183 (1986).
5. M.A. Hossai, and K. Mohammad, Jpn. J. Appl. Phys. **27**, 1531 (1988).
6. I. Pop and T. Watanabe, Int. J. Eng. Sci. **32**, 1903 (1994).
7. M. Acharya, G.C. Dash, and L.P. Singh, J. Phys. D: Appl. Phys. **28**, 2455 (1995).
8. M.A. Hossain and R.I.M.A. Rashid, J. Phys. Soc. Jpn. **56**, 97 (1987).
9. E.M. Aboeldahab and E.M.E. Elbarbary, Int. J. Eng. Sci. **39**, 1641 (2001).
10. H.S. Takhar, S. Roy, and G. Nath, Heat and Mass Transfer **39**, 825 (2003).
11. V.M. Soundalgekar and H.S. Takhar, Modelling, Measurement and Control **B51**, 31 (1993).
12. H.S. Takhar, R.S.R. Gorla, and V.M. Soundalgekar, Int. J. of Numer. Meth. Heat Fluid Flow **6**, 77 (1996).
13. M.A. Hossain and H.S. Takhar, Heat and Mass Transfer **31**, 243 (1996).
14. E.M. Aboeldahab, Heat and Mass Transfer **41**, 163 (2004).
15. R. Muthucumaraswamy and G.S. Kumar, Theor. Appl. Mech. **31**, 35 (2004).
16. M. Kinyanjui, J.K. Kwanza, and S.M. Uppal, Energy Conserv. Manag. **42**, 917 (2001).
17. K.R. Rajagopal, Acta Mechan. **48**, 233 (1983).
18. M.K. Chowdhury and M.N. Islam, Heat and Mass Transfer **36**, 439 (2000).
19. A.R. Bestman, Int. J. Numer. Meth. Eng. **21**, 899 (1985).
20. G.W. Sultan and A. Sherman, *Engineering Magnetohydrodynamics* (McGraw-Hill, New York, 1965).
21. R. Muthucumaraswamy and A. Vijayalakshmi, Theor. Appl. Mech. **32**, 223 (2005).

Received 16.03.07

ЕФЕКТ ХОЛЛА ДЛЯ МАГНІТОГІДРОДИНАМІЧНОГО КОНВЕКТИВНОГО ПОТОКУ В'ЯЗКОПРУЖНОЇ РІДИНИ, ЩО ОБТІКАЄ НЕСКІНЧЕННУ ВЕРТИКАЛЬНУ ПЛАСТИНУ, З ВРАХУВАННЯМ МАСОПЕРЕНОСУ ТА ВИПРОМІНЮВАННЯ

Р.С. Чодхарі, П. Джейн

Р е з ю м е

Досліджується нестаціонарний гідромагнітний потік в'язкопружної рідини від випромінюючої вертикальної пористой пластини з урахуванням масопереносу та струму Холла.

Задачу розв'язано аналітично. Розв'язки у замкнутому вигляді одержано для розподілів швидкості, температури, концентрації, зсувного напруження та швидкостей тепло- і масопереносу. Досліджено вплив різних параметрів (параметра Холла, магнітного параметра, коефіцієнта в'язкопружності, частоти і т.д.) на поле потоку.